THE USE OF NMR SPECTROSCOPY TO VALIDATE NMR LOGS FROM DEEPLY BURIED RESERVOIR SANDSTONES

H. Rueslåtten, T. Eidesmo, K.A. Lehne and O.M. Relling
Statoil Research Centre, Postuttak, N-7005 Trondheim

ABSTRACT

A Lower Jurassic deeply buried sandstone oil reservoir offshore Mid Norway was logged with NUMAR's MRIL-C tool. The NML data have been compared with standard logs as well as laboratory NMR and standard petrophysical core measurements. The two formations studied are in the oil zone, Formation A being characterised by an extensive distribution of pore lining chlorite, while asphalt staining is observed in the pores of cleaned Formation B samples. These characteristics are also recognised on the NMR T_1 data at irreducible water saturation with n-decane. Formation A samples is clearly water-wet while samples from Formation B show a mixed-wet behaviour.

A good match is found between NMR derived and measured porosities and saturations of the core plugs. The detrimental effect of chlorite on the T_2 relaxation is demonstrated by strong reduction of relaxation times for the longest T_2 components. Under-estimation of porosity (MPHI) from the NML data is related to the oil saturation of the logged formation. This phenomenon is attributed to a lower hydrogen index in the oil phase and diffusional processes induced by the applied magnetic field gradient. The under-estimation of porosity leads also to a general under-estimation of permeability. The fraction of bound water (BVI) derived from the NML data is lower in the mixed-wet formation This compensates to some extent for the underestimated porosity in the permeability estimates. It is further suggested that the BVI/MPHI ratio may be used as a wettability indicator.

INTRODUCTION

A deeply buried Lower Jurassic sandstone oil reservoir offshore Mid Norway is evaluated. The reservoir quality is controlled by sedimentary facies variations, primary sand quality and diagenesis. In general, the reservoir quality becomes progressively poorer with depth. High porosity is preserved in some reservoir units due to extensive diagenetically developed grain coating chlorite which has ceased the quartz overgrowth.

Most of the hydrocarbons are found in low permeable formations (0.001 to 10mD). It is therefore of crucial importance to distinguish between producing and non-producing sand. The definition of producing sand (or net sand) is based on permeability criteria, and for offshore fields the commonly used cut-off values for gas and oil bearing formations are 0.05mD and 0.1mD, respectively. Cut-off values based on porosity cannot be applied here because the correlation between porosity and permeability is poor. The estimates of permeability from the standard logs are therefore highly uncertain.

For these reasons it was decided to log the well with NUMAR's MRIL-C NMR logging tool, and to use core analysis for calibration. The new generation of Nuclear Magnetic Logging (NML) tools have generated much interest in the petroleum industry, as they provide a potential for obtaining information regarding porosity, permeability, free and bound fluids - and from this obtaining better estimates on the producibility of reservoir zones.

The aim of this paper is to describe the experiences gained by using NML in combination with a suite of standard logs and core data to establish porosity, irreducible water saturation (Swi), permeability and residual hydrocarbon saturations in the reservoir zones.

T1 MEASUREMENTS

NMR longitudinal relaxation time (T_1) for fully water saturated rocks is related to the pore size distribution and permeability of sandstones (Kenyon *et al.*, 1986; Howard *et al.*, 1990) The magnetic decay *g(t)* can be described as a sum of exponential terms according to the equation:

$$g(t) = \sum_{i=1}^{n} f_i e^{-\frac{t}{T_{1i}}} + \beta(t) \qquad (1)$$

where T_{1i} is the longitudinal relaxation time for pores of characteristic size i, f_i is the volume fraction of this pore size class, n is the number of exponential terms (usually two to four) and $\beta(t)$ is the noise inherent in the data.

For rocks saturated with two fluids (wetting and non-wetting) the relaxation behaviour is more dominated by the wettability conditions than by the pore sizes. In this case the magnetic decay (g(t)) can be described by a sum of four exponential terms;

$$g(t) = f_{iw}e^{-\frac{t}{T_{1iw}}} + f_{w}e^{-\frac{t}{T_{1w}}} + f_{io}e^{-\frac{t}{T_{1o}}} + f_{o}e^{-\frac{t}{T_{1o}}} + \beta(t) \qquad (2)$$

where T_{1iw} and T_{1io} are the relaxation time for wetting water and oil, respectively, and T_{1bw} and T_{1bo} are the relaxation time for bulk water and oil, respectively. The magnetic decay will be even more complicated when crude oil is confined in the rock, as the crude oil consists of a mixture of chemical compounds which give a number of T_1 bulk components and self diffusion constants (Rueslåtten et al., 1994).

THE NML TOOL AND T2 MEASUREMENTS

NUMAR's MRIL-C tool has a 600 mm long permanent magnet which generates a static magnetic gradient field into the near wellbore formation (Chandler et al., 1994). By tuning the Larmor frequency, the measured volume is defined at a distance from the wellbore. This sensed rock volume is supposed to be in the outer limit of the invaded zone, and the measurements are therefore assumed to be less affected by invaded mud filtrate (Mardon et al., 1996). The invasion of mud filtrate depends, however, on a number of factors, such as rock characteristics, confined fluids, mud type and pressure. Due to this, the influence of mud filtrate will vary and should not be neglected.

The MRIL-C tool measures T_2 which is relatively fast and easy to conduct compared to T_1 with respect to operational limitations, but the T_2 relaxation process is more complicated. A T_2 relaxation process measured with the so called Carr-Purcell-Meiboom-Gill (CPMG) pulse sequence can be described by Equation 3;

$$\left(\frac{1}{T_2}\right)_{Liquid} \cong \rho\left(\frac{S}{V}\right) + \left(\frac{1}{T_2}\right)_{Bulk} + \frac{1}{3}(\tau\gamma\nabla B)^2 D \qquad (3)$$

where S/V is the Surface to Volume ratio, ρ is the surface relaxation strength, τ the inter echo spacing, γ the gyromagnetic ratio for hydrogen, ∇B the magnetic field gradient and D the self diffusion constant of the fluid confined in the pore space.

The first term on the right hand side states that the T_2 relaxation is dependent on the fluid-rock interactions given by ρ and the ratio S/V which also can represent the pore sizes in the rock.

The second term states that the T_2 relaxation depends on the bulk T_2 relaxation of the confined fluid. Generally, the T_2 relaxation time of the bulk fluid increases with temperature and reduced viscosity, and the viscosity of a crude oil decreases with increasing Gas Oil Ratio (GOR) and temperature.

The third term in Eq. 3 states that all other parameters being constant, the T_2 relaxation rate will increase with increasing self diffusion in the fluid. This is caused by hydrogen spins moving into regions of different frequency. To reduce the effect of the diffusional motion one can reduce either the magnetic gradient ∇B and/or τ. It should be noted that the third term in Eq. 3 does not influence on T_1 relaxation.

The interpretation of MRIL-C is based on stacked measurements each consisting of a number of spin echo pulses with τ equal to 1.2 msec and a typical repetition time $\Delta t = 6$ sec. The repetition time is the time between each 90 degree pulse in the CPMG pulse sequence. The resulting curve y(t) can be represented by Equation 4 (Prammer, 1994).

$$y(t) = \int_{T_2=0}^{T_{2bulk}} P(T_2)e^{-\frac{t}{T_2}}dT_2 + \varepsilon(t) \qquad (4)$$

Equation 4 describes a system with a continuous T_2 distribution and a noise signal $\varepsilon(t)$. To describe the system, $P(T_2)$ and the corresponding T_2's are found by fitting y(t) (given by Equation 5) to the raw data.

$$y(t) = \sum_{i=1}^{8} P_i e^{-\frac{t}{T_{2i}}} \qquad (5)$$

To simplify the fitting procedure the T_2's are predefined leaving the corresponding P_i's as unknowns (Prammer, 1994). The T_2's are predefined to 4, 8, 16, 32, 64, 128, 256 and 512 msec, respectively. The resulting T_2 distribution is given by the P_i's (or bins). The P_i's are given in Porosity Units (PU) and the sum of the 8 P_i's defines the porosity of the rock (MPHI).

Based on the fact that the short T2 components most likely are associated with bound fluid, the "bound fluid" (BVI) is commonly defined by the sum of the first 3 P_i's, indicating a cut-off between "free fluid" (FFI) and BVI between 16 and 32 msec (Miller et al. 1990). In the investigated North Sea wells the best result is obtained by using the first 4 P_i's to represent BVI.

The permeability estimations presented in this paper is based on Equation 6 (Prammer, 1994).

$$K = C * MPHI^4(\frac{FFI}{BVI})^2; C = 10^{-4} \quad (6)$$

BVI is defined by the sum of the first 3 P_i's (bins)

SEDIMENTS AND DIAGENESIS

Formation B consists of shallow marine tidal shoal and foreshore sandstones, while Formation A (above) consists of progradational sandlobes redistributed by tidal processes and deposited in a shallow basin. The diagenetic processes are decisive for the reservoir quality in this deeply buried sandstones. Quartz cementation increases with depth, and at temperatures exceeding 80 °C this cementation process is in general controlled by temperature (Oelkers et al., 1996).

The most important process for preserving porosity and permeability in this reservoir is the extensive distribution of grain coating chlorite. The chloritization, which is most pronounced in Formation A, is the main reason for the preservation of producibility in these oil bearing sandstone formations. The onset of the chloritization process is not known, but porosities up to 25% encountered within the cored interval indicates that the quartz overgrowth must have ceased at temperatures between 90 and 100 °C (Bjørkum 1996). Consequently, the chloritization must have developed at these temperatures.

At temperatures above 130 °C a fibrous pore-bridging illite is commonly found; also in zones with extensive grain coating chlorite. This illitization process does not influence significantly on porosity but it is damaging to permeability. The illitization process is based on dissolution of potassium feldspar and kaolinite, and consequently a secondary porosity is developed. This secondary porosity is, however, probably of less importance for conducting fluid flow due to its patchyness and the blocking effect of new formed illite.

EXPERIMENTAL PROCEDURES

Core plugs: In the cored interval, a large number of core plugs were drilled out and tested for porosity and permeability according to standard laboratory procedures; He-porosimetry and Klinkenberg corrected air permeability. Five core plugs were selected for further testing. They are supposed to represent the main units in the cored interval of the well. The plugs measuring 38 mm in diameter and 70 mm long, were drilled out and run through a comprehensive experimental programme including petrophysical and NMR measurements and petrographical analyses. End cut-offs from the core plugs were used for thin sections and XRD analysis.

Fluids: The fluids used in the experimental programme are crude oils from Formation A and B degassed at 60°C, and synthetic brine prepared according to analysis of the formation water. Decane was used for some of the NMR experiments in order to simplify the interpretations. The core plugs were run through the following experimental sequence:

Experimental sequence:
(i) Freshly received core plugs were flooded with crude oil to establish irreducible water saturation; "Swi crude".
NMR measurements performed at "Swi crude".
(ii) Flooding with synthetic formation water to residual oil saturation; "Sor crude".
NMR measurements performed at "Sor crude".
(iii) Flooding the samples with n-decane to irreducible water saturation; "Swi decane".
NMR measurements performed at "Swi decane".
(iv) Extraction of water performed by the Dean & Stark method. The results are used to calculate water saturation.
(v) Cleaning of the core plugs by Soxhlet extraction in toluene and methanol, followed by drying at 80 °C for 64 hours and then placed in a desiccator containing silica gel.
(vi) Measurements of helium porosity (ϕ_{He}) and Klinkenberg corrected gas permeability (k_L).

All experiments were carried out at ambient conditions.
NMR Measurements: Laboratory NMR measurements were performed using a Resonance - MARAN-2 NMR Spectrometer at a proton resonance frequency of 2.04 MHz. The T2 relaxation curves were measured using a Repetion Time (RT) of 10sec, number of echoes 8100, and CPMG inter echo spacing (τ) 350μs. Spin lattice relaxation curves (T_1) were measured using a (π - τ -

$\pi/2$) inversion recovery sequence. The π and $\pi/2$ pulses were approximately 34μs and 17μs, respectively, (tuned according to core susceptibility). Thirty data points were recorded in order to cover the entire T_1 relaxation curve. The temperature of the sample holder was controlled at 30°C.

RESULTS AND DISCUSSION

Mineralogy: The rock samples are predominantly composed of quartz, feldspars, carbonates and various amounts of clay minerals; mainly chlorite. Iron bearing cementing minerals like ankerite, pyrite and siderite are also abundant in some of the samples (Table 1). The thin sections from Formation A reveal a continuos porelining of chlorite covering all pore surfaces (Fig. 1). The continuity of the pore system is apparently good, but chlorite growing in the pore throats is detrimental to permeability. The Formation B samples are characterised by higher maturity (up to 95% quartz) and lower clay content than the A samples. Sample B1 is characterised by abundant loadbearing ankerite. A striking feature is a dark rim of asphalt-like material covering much of the pore surfaces in the B samples (Fig. 1). This material has "survived" the cleaning procedure and the injection of epoxy resin. The asphalt coating indicates a more oil-wetting behaviour of the B formation, and the oil-wetting may also have contributed to the preservation of porosity during burial.

Petrophysical data: The porosity of the samples varies between 0.12 and 0.20, and air permeability (k_L-Klinkenberg corrected) varies between 4.1 mD and 31.9 (Table 2). High irreducible water saturations with crude oil ("Swi crude") were encountered for the samples. The highest values are found for the A samples (up to 0.555), This is attributed to their higher clay contents. Residual oil saturation ("Sor crude") varies from 0.153 to 0.328, but no significant differences can be seen between the A and the B samples.

NMR T_1 measurements: The porosity of the 5 rock samples determined by NMR gives a very good match with the measured values (Table 2). Crude oils give a bulk multicomponent signal on NMR (Table 3). This complicates the interpretation of the NMR data with respect to deducing information about the fluid behaviour and distribution within the pore system. In order to obtain a more well defined NMR response, the crude oil was displaced by n-decane to an irreducible water saturation ("Swi decane"). The n-decane is characterised by only one T_1 component on 1.5 sec.

The NMR relaxation data were analysed using the multiexponential model with three exponential terms (Eq. 1). The effect of wettability is clearly demonstrated by the contrast in T_1 relaxation behaviour for the A and B samples, see Fig. 3. The magnitudes of the longest T_1 components of the A samples are approaching 1.5 sec which match the T_1 relaxation time of bulk decane. This is interpreted as an indication of a strongly water-wet system with decane relaxing as bulk oil in the pore space, shielded from the pore walls by wetting water films (Øren *et al.*, 1994). The longest T_1 components for the two B samples are shorter than the bulk relaxation time for decane, indicating a mixed wettability. This is in accordance with the thin section observations of asphalt coatings on the pore walls.

Furthermore, the intensities of the longest T_1 components match the oil saturations of both A and B samples, despite the shorter relaxation times of the B samples. This is illustrated on Fig. 4 which shows the measured water saturation versus the intensities of the two shortest T_1 components.

The mixed wettability character of the B samples is also revealed by the larger magnitudes of the longest T_1 components at residual crude oil saturation (Sor crude) (Fig. 3); indicating that some of the water is shielded from the pore surfaces by hydrocarbon films and relaxes as "bulk" water with a T_1 relaxation time of 3.5 sec. The NMR data acquired at Swi and Sor with crude oil is more difficult to interpret quantitatively due to the multicomponent relaxation signal from the crude oil and its interference with the water relaxation signals from the various pore size classes (Table 3).

The noise in the data, $\beta(t)$ (Eq.1 and 2), is in general low and evenly distributed along the entire relaxation curve. This is illustrated on Fig. 11 where the difference between measured and processed data is plotted versus time.

NMR T_2 measurements: The magnitudes of the longest T_2 components at the various oil/water saturations show a pattern of mutual size relations which is different to the corresponding longest T_1 components, see Fig. 5. This is particularly conspicuous for the A samples at Swi with decane. *Their longest T_2 components are now shorter than those of the B samples.*

It is suggested that the reason for this increase in relaxation rate for the A samples is the pore-lining

chlorite. The siderite and pyrite in sample A1 may also have contributed to this effect (Murphy, 1995), but the higher surface area of the pore lining chlorite in contact with the pore fluids is propably the most important factor. The physical reason for the faster T_2 decay of the non-wetting n-decane must be that the paramagnetic minerals are causing heterogeneities in the applied magnetic field and inducing internal magnetic field gradients on the pore level due to magnetic susceptibility contrasts between the rock grains and the pore fluids. These internal field gradients are promoting diffusional movements of the decane molecules out of the frequency domain, resulting in a faster T_2 decay. In fine grained porous material (e.g. chlorite) only small contrasts in susceptibility is needed for internal gradients to dominate the relaxation rate (LaTorraca et al., 1995). The wetting water phase is interacting with the pore surface, and it is assumed that it is not influenced so strongly by the gradient fields.

A result of the faster T_2 decay of the non-wetting phase due to paramagnetic minerals is that the differences in wettability between the A and B samples are more difficult to see on the T_2 data.

Furthermore, the intensities of the shortest T_2 components alone (out of 3 exponential terms) match the water saturation, meaning that decane is now contributing to both the longest and the intermediate T_2 components, see Fig. 6.

Fluids in intermediate wet rocks will have at least four different relaxation characteristics: oil and water without rock contact ("bulk" fluids), and oil and water with rock contact at shorter relaxation times. For this reason, the NMR data were also interpreted using the multiexponential model with four terms (Table 3). In order to investigate the possibility of isolating the relaxation component for "bulk" brine at Swi and Sor with crude oil, the longest component in the four exponential representation was fixed at the bulk relaxation time for water (3.5 sec). The intensity of this component should then indicate the amount of brine in the sample which is not in contact with the rock surface. The calculations gave intensity values between 1.2 and 8.2% at Swi crude, and 1.2 to 13.9% at Sor crude. Highest values were obtained for the two mixed wet B samples, see Fig. 7. The rest of the residual water is expected to reside in small water wet pores and as pendular water with short relaxation times reflected in the shortest T_2 component.

Estimated permeabilities of the core plugs based on NMR data is given in Table 2. The calculated values deviate from the measured ones, and this is particularly the case for the B samples. This is due to lower BVI values (less bound water) in these samples which causes higher FFI/BVI values and consequently higher estimated permeabilities. Note that the poor correlation between porosity and permeability in these rocks will strongly influence the NMR permeability estimations.

Calculation of BVI: In order to make comparisons with the MRIL-C logging data the experimental T_2 data were also calculated into P_i's (or "bins") according to Eq. 5 (Table 3). A comparison between the shortest component in the four exponential representation of the T_2 data (with the longest component fixed at 3.5 sec) and the sum of the three first bins (=BVI) are shown on Fig. 8 together with the measured irreducible water saturation with crude oil. As is evident from the figure, there is a rather good match between these three parameters, which supports the idea to use the three first bins of the NML data to represent the bound water.

It should be mentioned, however, that by adding the bulk water (in Fig. 7) to the bound water (in Fig. 8) the total water saturation is overestimated, particularly for the B samples. This is explained by small amounts of oil contributing to the shortest T_2 component for the mixed-wet B samples. An analogous result is obtained with n-decane at Swi. The NML data from the well show similar effects.

MRIL-C LOG DATA

NML porosity and water saturation: A general under-estimation of porosity by the NML (MPHI) is observed throughout the oil zone as compared to the porosity (PHIF) derived from the standard density log. In the water zone, however, a good match is found for the two logs (Eidesmo et al., 1996). The influence of water saturation on MRIL-C derived porosity (MPHI) is shown in Fig. 9. A clear trend seem to emerge from the figure. The under-estimation of porosity in Formation A and B is in the order of 5 Pore Units (PU) on average (around 1/3 of the total porosity). The measurements of fully water saturated formation show a good match for the two logs, but an increased difference in porosity is seen with increasing oil saturation. It is therefore concluded that the under-estimation of porosity is connected to the oil phase. The hydrogen index in the reservoir oil is lower than one, and this is assumed to be an important factor to the under-estimation of porosity.

It is also suggested that the applied magnetic field gradient is causing the non-wetting oil to diffuse out of the frequency domain during the relaxation process, and that this also may lead to a reduced porosity estimation. If this hypothesis is to be valid, a less pronounced effect on the mixed-wet Formation B would be expected. This is not seen, however, and it is argued that in this mixed wetted rocks the majority of the oil volume is not in contact with the pore surfaces (Rueslåtten et al. 1994). This may also be inferred from the discussion above regarding the low volume of bulk water (at Swi crude) represented in the longest T2 component (Fig. 7). A shorter repetition time (τ) in the logging procedure of T_2 may improve the detection of oil (Eq. 3).

The experimental results regarding the effect of chlorite (and other paramagnetic minerals) on the T_2 experiments may also be inferred from Fig. 9. A larger spread of the data points is seen in the clay rich A Formation compared to the B Formation.

Estmation of permeability: The NML permeability is calculated by applying Eq. 6, and the input parameters are porosity and the FFI/BVI ratio. The under-estimation of the volume of oil by NML will lead to lower porosities (MPHI) and lower FFI/BVI ratios; both of which lead to an under-estimation of permeability. The mixed-wet B Formation gives in general, lower BVI values (less bound water) which improve the estimated permeabilities. This is demonstrated by the core plug experiments (Table 2).

Wettability: The more oil-prone wettability of the B Formation is seen by comparing the BVI/MPHI ratios with the water saturation (Sw) derived from the resistivity log, see Fig.10. The data points from Formation B are characterized by having higher Sw/(BVI/MPHI) ratios compared to Formation A, indicating that less bound water is present in the B Formation.

CONCLUSIONS

A deeply buried sandstone oil reservoir offshore Mid Norway is evaluated. The two formations studied are localised in the oil zone, and Formation A is characterised by an extensive distribution of pore lining chlorite, while an asphalt staining in the pores is observed in the thin sections from the Formation B samples. These characteristics are also recognised in the NMR T_1 data at irreducible water saturation with n-decane, by the magnitude of the longest T1 components being close to the relaxation time of bulk n-decane for the A samples (water-wet) and lower for the B samples (mixed-wet). The similarly derived long components from the T_2 data show the opposite trend. It is suggested that the faster T_2 magnetisation decay is caused by the chlorite content in the A samples. The chlorite causes heterogeneities in the applied static magnetic field and internal magnetic field gradients on the pore scale. The non-wetting n-decane is affected more by these internal field gradients than the wetting fluids which are interacting with the pore walls. These effects are not seen on the NMR T_1 data.

A good match is found between the measured irreducible water saturations and the intensities of the shortest T_1 and T_2 components. The sum of bound and bulk water derived from the NMR components is slightly higher than the measured water saturation for the mixed-wet samples, indicating that some oil in oil-wetting pores is contributing to the shortest components in these samples, and consequently interpreted as BVI.

The observed under-estimation of NML derived porosity (MPHI) is related to the oil saturation. It is suggested that this under-estimation is mainly due to an influence on the non-wetting phase; mainly the oil.

Permeability is generally under-estimated in the oil zones due to the under-estimation of porosity (MPHI). In the mixed-wet zones a lower BVI may compensate for the under-estimated porosity in the calculation of permeability. In this case the BVI will represent both wetting water and oil, and FFI will represent non-wetting (bulk) water and oil. It is suggested that the more oil-prone wettability in Formation B is seen by higher Sw/(BVI/MPHI) ratios in the wireline log data.

Although NML data have a high potential in providing useful reservoir information, the interpretation of the data is, however, far from straightforward. Rigorous validation under a wide variety of reservoir conditions using NMR-spectroscopy and other core analyses is still required before the data can be widely applied to formation evaluation.

ACKNOWLEDGEMENT

The authors would like to thank Den norske stats oljeselskap a.s (Statoil) for permission to publish this paper.

REFERENCES

Bjørkum, P.A., 1996, How important is pressure in controlling dissolution of quartz in sandstones? Journ. Sedm. Research. p. 147-154.

Chandler, R.N., Drack, E.O., Miller, M.N. and Prammer, M.G., 1994, Improved Log Quality With a Dual-Frequency Pulsed NMR Tool, presented at the 69th Annual Technical Conference and exhibition of the Society of Petroleum Engineers, New Orleans, September 25-28.

Eidesmo, T., Relling, O.M., Rueslåtten, H., 1996, NMR Logging of Mixed-Wet North Sea Sandstone Reservoirs To be presented at the 37th Annual SPWLA Symposium, New Orleans, June 16-19.

Howard, J.J., Kenyon, W.E. and Straley, S., 1990, Proton Magnetic Resonance and Pore-Size Variations in Reservoir Sandstones. SPE 10600. SPE Annual Tech. Conf. Exhib., New Orleans, Sept. 1990.

Kenyon, B., Day, P.I., Starley, C., and Willemsen, J.F., 1986, Compact and Consistent Representation of Rock NMR Data for Permeability Estimation. SPE 15643. SPE Annual Tech. Conf. Exhib., New Orleans, Oct. 1986.

LaTorraca, G.A., Dunn, K.J. and Bergman, D.J., 1995, Magnetic Susceptibility Contrast Effects on NMR T2 Logging, SPWLA 36th Annual Logging Symposium, Paris, June 26-29.

Mardon D., Prammer M.G., Coates G.R.: Characterization of Light Hydrocarbon Reservoirs by Gradient-NMR Well Logging. To be published in Magnetic Resonance Imaging, 1996.

Miller, M.N., Paltiel, M.E., Granot, J. and Bouton, J.C., 1990, Spin Echo Magnetic Resonance Logging: Porosity and Free Fluid Index Determination, presented at the 65th Annual Technical Conference and exhibition of the Society of Petroleum Engineers, New Orleans, September 23-26.

Murphy, D.P., 1995, NMR logging and core analysis - simplified, World Oil, April 1995.

Oelkers, E.H., Bjørkum, P.A. and Murphy, W.M., 1996, A petrographic and computional investigation of quartz cementation and porosity reduction in North Sea sandstones. American Journal of Science.

Prammer, M.G., 1994, NMR pore size distributions and permeability at the well site, presented at the 69th Annual Technical Conference and exhibition of the Society of Petroleum Engineers, New Orleans, September 25-28.

Rueslåtten, H., Øren, P-E., Robin, M., Rosenberg, E. and Cuiec, L., 1994, A Combined Use of CRYO-SEM and NMR-Spectroscopy for Studying the Distribution of Oil and Brine in Sandstones, presented at the SPE/DOE Ninth Symposium on Improved Oil Recovery, Tulsa, April 17-20.

Øren, P.-E., Rueslåtten, H.G., Skjetne, T. and Buller, A.T., 1994, Some Advances in NMR Characterization of Reservoir Sandstones. Proc. North Sea Oil and Gas Reservoirs-III, Norwegian Institute of Technology, Trondheim.

Table 1. Mineralogical composition of core plugs. Semi-quantitative XRD analysis. Small amounts of kaolinite are included in the chlorite fraction. (*)Ankerite.

Sample No.	Depth (m)	Kvarts	Feldspar	Illite/Mica	Calcite	Siderite	Pyrite	Chlorite
A1	X189	30.6	6.0	4.0	1.7	43.9	3.0	10.8
A2	X199	69.3	7.5	1.6	9.9	-	0.5	11.3
A3	X209	73.6	5.6	0.6	8.1	1.8	0.4	9.7
B1	X234	65.6	2.1	1.1	31(*)	-	-	0.1
B2	X237	95.0	2.1	0.5	-	-	-	2.5

Table 2. Petrophysical and NMR data for 5 reservoir sandstones samples tested with gas in dry condition and at irreducibel water saturation with crude oil ("Swi crude"). Calculated permeability from NMR data at "Swi crude" is based on the equation $k_{NMR} = 10^{-4} MPHI^4 (FFI/BVI)^2$.

Sample No.	Porosity (ϕ_{He})	Perm. k_L (mD)	Swi crude (frac.)	Sor crude (frac.)	Porosity (ϕ_{NMR}) (Swi cr.)	Perm. k_{NMR} (mD) (Swi cr.)
A1	0.200	31.9	0.555	0.153	0.194	8
A2	0.149	4.1	0.387	0.328	0.149	4
A3	0.180	10.2	0.496	0.261	0.178	8
B1	0.123	10.9	0.193	0.265	0.117	42
B2	0.148	19.7	0.313	0.242	0.147	47

Table 3. NMR data for the five core plugs at three various saturations. The T_2 relaxation times are in msec. The numbers in brackets are the intensities of each component. * Longest T_2 component fixed at 3500 msec.

Sample No.	Sw	T_2 Comp. 1	T_2 Comp. 2	T_2 Comp. 3	T_2 Comp. 4
A1	Swi crude: 55.5%	5 (52.7%)	56 (22.3%)	259 (22.9%)	3500* (2.1%)
A2	Swi crude: 38.7%	6 (49.6%)	62 (24.5%)	251 (24.7%)	3500* (1.2%)
A3	Swi crude: 49.6%	5 (49.8%)	59 (21.8%)	294 (24.7%)	3500* (3.7%)
B1	Swi crude: 19.3%	5 (15.0%)	44 (32.0%)	381 (44.8%)	3500* (8.2%)
B2	Swi crude: 31.3%	10 (28.9%)	88 (21.2%)	453 (41.8%)	3500* (8.1%)
Formation A Crude oil (T_1)	Bulk	1.1 (4.3%)	150 (41.1)	820 (54.6%)	-
Formation B Crude oil (T_1)	Bulk	1.2 (4.2%)	246 (30.8%)	1070 (65.0%)	-

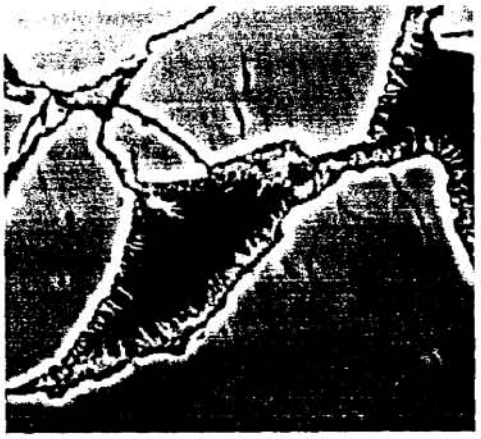

Figure 1. SEM micrograph of thin section (Sample A2) showing porelining chlorite. Image size 0.15mm.

Figure 2. Photomicrograph of thin section (Sample B2) showing asphaltene staining on pore surfaces. Image size 0.15mm.

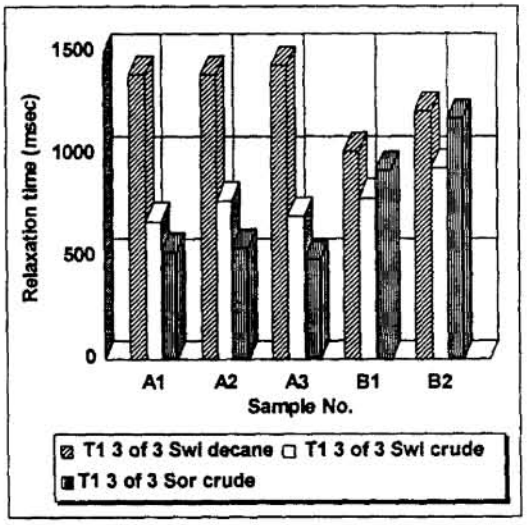

Figure 3. The longest T_1 component out of 3 exponential terms at irreducible water saturation with n-decane (Swi decane) and crude oil (Swi crude), and at residual crude oil saturation (Sor crude).

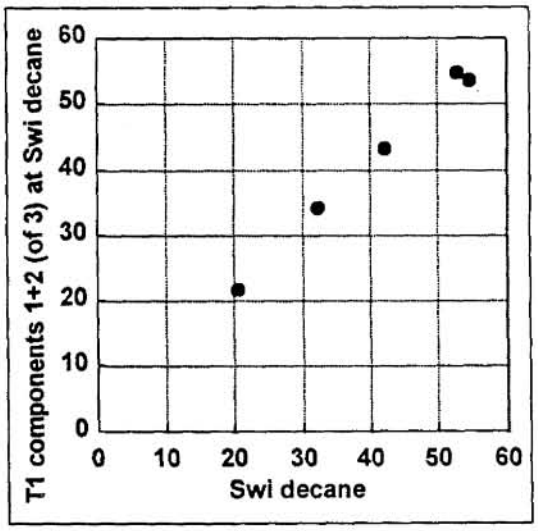

Figure 4. Irreducible water saturation (Swi decane) versus the intensities of the two shortest T_1 components.

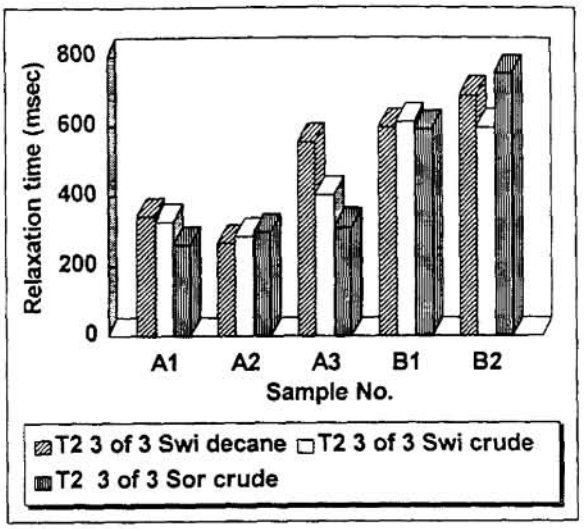

Figure 5. The longest T_2 component out of 3 exponential terms at irreducible water saturation with crude oil (Swi crude) and n-decane (Swi decane), and at residual crude oil saturation (Sor crude).

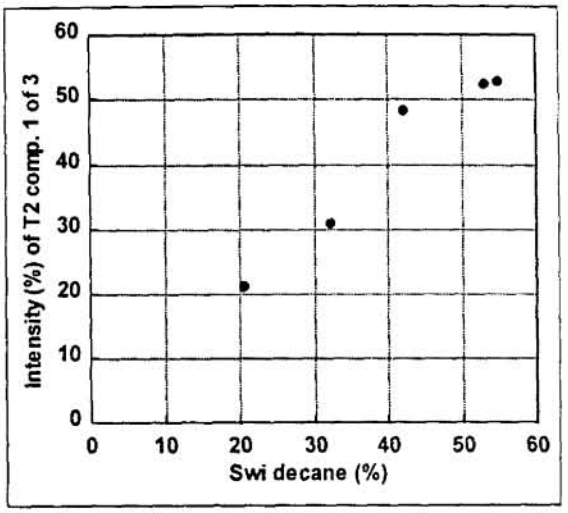

Figure 6. Irreducible water saturation (Swi decane) versus the intensities of the shortest T_2 component.

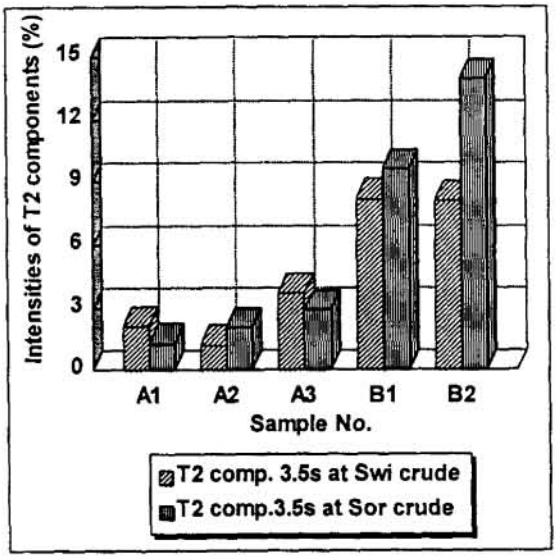

Figure 7. Intensity of longest T_2 component fixed at 3.5 sec and four exponential terms; at irreducible water saturation with crude oil (Swi crude) and at residual crude oil saturation (Sor crude).

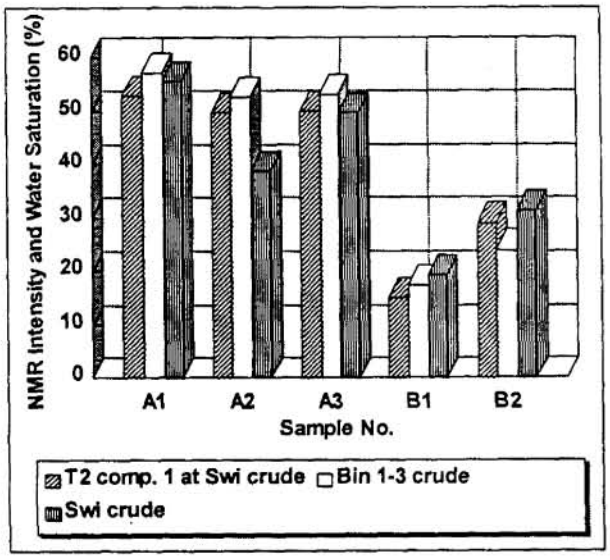

Figure 8. Intensity of shortest T_2 component at Swi crude; BVI represented by the sum of bin 1-3; and measured irreducible water saturation with crude oil (Swi crude).

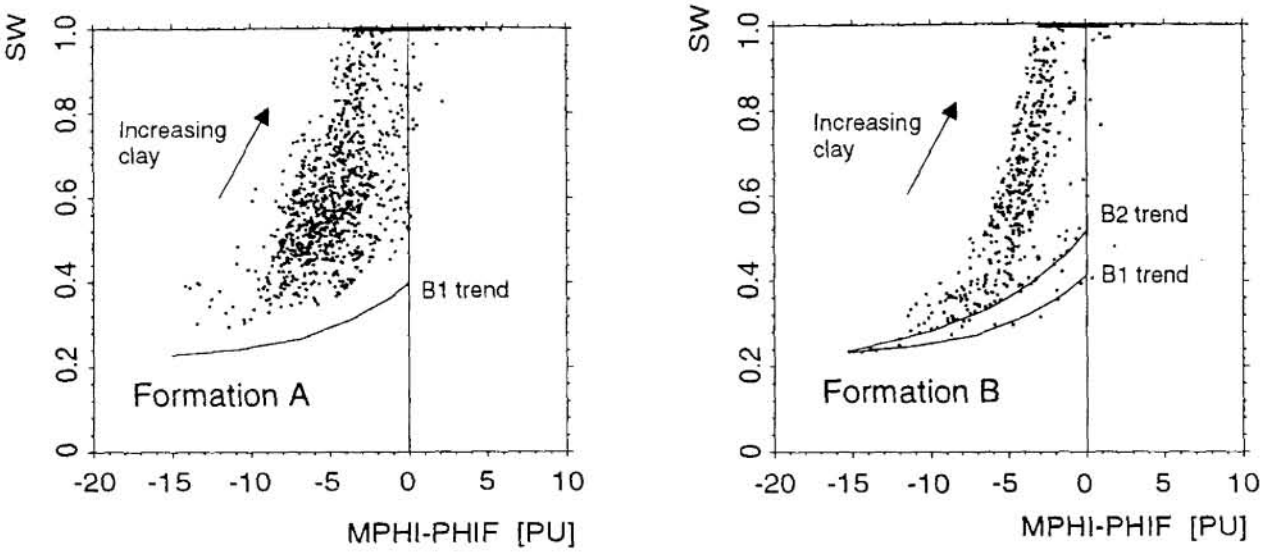

Figure 9. The difference between NMR derived porosity (MPHI) and standard log porosity (PHIF) versus water saturation (SW) derived from resistivity log.

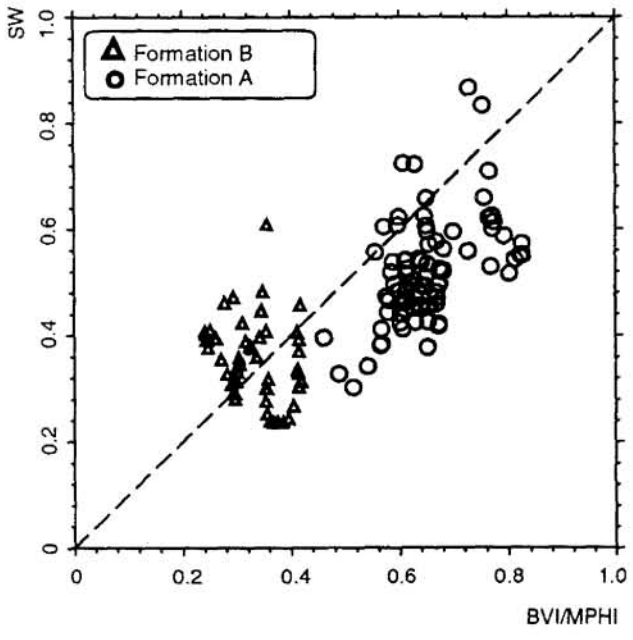

Figure 10. Relation between the BVI/MPHI ratio and the water saturation (SW) derived from resistivity log.

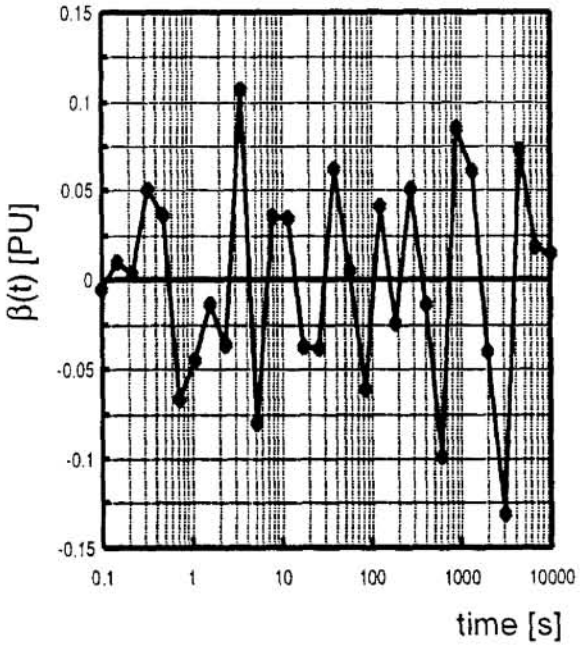

Figure 11. The figure depicts how β(t) varies with time for sample B2.